Check for updates

Received: 24 September 2024 | Revised: 5 November 2024 | Accepted: 27 December 2024

DOI: 10.1002/pc.29460

RESEARCH ARTICLE

Polymer COMPOSITES WILEY

Evaluation of the effect of triphenyl phosphate on hemp fiber-reinforced polycarbonate composites for 3D printing applications

Irem Ceylan Engin[1] | **Nese Cakici Alp**[1] | **Ayse Aytac**[2,3]

[1]Department of Architecture, Kocaeli University, Architecture and Design Faculty, Kocaeli, Turkey

[2]Department of Chemical Engineering, Kocaeli University, Engineering Faculty, Kocaeli, Turkey

[3]Polymer Science and Technology Programme, Kocaeli University, Kocaeli, Turkey

Correspondence
Irem Ceylan Engin, Architecture Department, Kocaeli University, Architecture and Design Faculty, 41300 Izmit/Kocaeli, Turkey.
Email: iremceylan-@hotmail.com

Funding information
Kocaeli Üniversitesi

Abstract

This study examined the effects of adding plasticizer to 3D printable hemp fiber-reinforced polycarbonate (PCH) composites to improve composite properties and facilitate the 3D printing process. The plasticizer or flame retardant, triphenyl phosphate (TPP), was added to the PCH composite at three different ratios (5%, 10%, and 20%). The characterization of composites was realized with Fourier-transformed infrared spectroscopy (FTIR), differential scanning calorimeter (DSC), thermogravimetric analysis (TGA), rheological analysis, tensile testing, limiting oxygen index (LOI), and scanning electron microscope (SEM) analyses. According to DSC results, while the glass transition temperature of pure PC was 148.44°C, it was reduced to 93.74°C with the addition of TPP. TGA analysis showed that PC has the best thermal resistance. The tensile test demonstrated that 20%TPP-containing samples exhibited a value of 59.52 MPa, representing a 38% increase compared to pure PC. Additionally, the LOI value of this sample is 32.4, increased by 12% compared to pure PC. Furthermore, SEM analysis showed that TPP reduced the gaps between the matrix and fiber. In general, the properties improved with an increase in TPP content. A composite was developed from a partially natural and more sustainable material, with improved properties and 3D printing processability compared to pure polycarbonate.

Highlights

- 10%TPP-added composite has demonstrated the best thermal resistance
- 20% TPP-added composite has 32.4 LOI and 59.52 MPa tensile strength values
- Adding hemp fiber to PC did not significantly change the T_g value
- 20% TPP addition to the composite reduced the T_g value by 63%.
- The 3D printing process has become easier with the increasing TPP ratio.

KEYWORDS

3D printer materials, alkali-treated-hemp fiber, FDM, plasticizer, polycarbonate, TPP

This is an open access article under the terms of the Creative Commons Attribution-NonCommercial-NoDerivs License, which permits use and distribution in any medium, provided the original work is properly cited, the use is non-commercial and no modifications or adaptations are made.
© 2025 The Author(s). *Polymer Composites* published by Wiley Periodicals LLC on behalf of Society of Plastics Engineers.

1 | INTRODUCTION

In recent times, the world has been facing an escalating ecological crisis due to issues such as increasing global warming, CO_2 emissions, and excessive energy consumption. The construction sector is accountable for 36% of overall energy consumption and contributes to 40% of carbon dioxide emissions.[1] Consequently, offering ecological solutions for architectural practices plays a crucial role in promoting environmental sustainability. Efforts to tackle these environmental challenges have led to research focused on eco-friendly materials and application methods that offer significant environmental advantages over traditional production techniques.

Eco-friendly materials are either fully or partially derived from biological sources (reinforcing material) and are utilized in a wide range of building applications.[2] Natural fibers (NFs), which are commonly used as reinforcement materials, are highly favored due to their abundance in nature, flexibility during processing, lightweight nature, cost-effectiveness, and enhanced mechanical properties in comparison to synthetic materials.[3–5] One promising matrix material for incorporating NFs as reinforcement is polymers. The use of NF-reinforced polymer composites (NFRPC) is increasingly being considered as a viable alternative to glass fiber-reinforced polymers in the construction industry due to its potential to reduce environmental impact.[6] The polymers employed in NFRPC can be classified as either thermoset or thermoplastic. In the case of thermoset NFRPCs, it is well-established that incorporating NFs, particularly hemp fiber, can significantly enhance the various properties of the composite.[7–9] Regarding the environmental benefits of NFRPCs, thermoplastic polymers stand out due to their ability to be recycled multiple times without undergoing degradation from heat, thus making them a more sustainable option for composites.[10] Common thermoplastic polymers utilized in NFRPCs include polyethylene (PE),[11] polylactic acid (PLA),[12] polypropylene (PP),[13] polystyrene,[14] polyvinyl chloride (PVC),[15] and polycarbonate (PC).[16] NFRPCs can incorporate NFs like bamboo, flax, jute, hemp, oil palm fruit bunch, banana, kenaf, sisal, cotton, coir, and ramie.[17–19] Among these, jute, sisal, flax, and hemp fibers present viable alternatives to traditional glass fiber- and carbon fiber-reinforced composites across a range of applications.[20,21] Research indicates that hemp and flax plants offer more increased stability for composites. For example, the tensile strength of jute fiber-strengthened PP is 23.56 MPa,[22] while it is 29.5 MPa for hemp fiber-strengthened PP.[23] Notably, flax fibers, unlike hemp fibers, mainly consist of low-molecular-weight pectin, which may result in a perceived coarse structure and potential surface imperfections.[24–26] It is well-established that in NFRPC, the characteristics of the composite are closely linked to the type of fiber used,[27] and it appears that using hemp fiber can enhance mechanical and morphological properties. Regarding sustainability, hemp boasts a growth rate of 3–9 times faster than other plants, and it can be cultivated in various regions, yielding more fiber per acre. Moreover, it exhibits higher CO_2 absorption capacity than all other existing plants.[28,29] Therefore, incorporating hemp fiber into the matrix not only improves composite properties but also contributes to environmental sustainability.

The use of NFRPC in construction presents environmental benefits, but it also carries undeniable environmental impacts when used with traditional manufacturing methods. Additive manufacturing (AM), often referred to as 3D printing, has the potential to improve sustainability compared to traditional techniques. 3D printers are powered by electricity, produce no emissions, and have reduced embodied energy, which can enhance a building's carbon footprint.[30–32] In comparison to traditional manufacturing, 3D printing can decrease production time by 70%, raw material usage by 70%, and waste materials by 60%.[33,34] Moreover, the layer-by-layer material addition in AM allows for the creation of intricate geometric shapes,[35] offering numerous advantages in the utilization of NFRPC with 3D printing.

According to the (ISO)/American Society for Testing and Materials (ASTM) 52900:2015 standard, there are seven types of AM processes. The most prevalent among these is fused deposition modeling (FDM), which is easily applicable to polymer and polymer composite materials.[35] The polymer materials utilized in FDM are polypropylene (PP), acrylonitrile–butadiene–styrene (ABS), polycarbonate (PC), and polylactic acid (PLA).[36,37] Extensive studies in the literature have focused on 3D printable NFRPCs obtained by reinforcing these polymers with various NFs. For instance, 3D printable NFRPC was manufactured by reinforcing PP with flax,[38] harakeke,[39] and hemp[40] fibers. ABS was reinforced with gongura roselle,[41] rice straw,[42,43] coconut,[44] jute,[45,46] oil palm,[47] and royal palm[48] fibers. PLA was paired with henequen,[49] agave,[50] sugarcane bagasse,[51] bamboo,[52] jute,[53] and hemp[54] fibers. Looking at the studies on PC, it was seen that 3D printable NFRPC was created by reinforcing with cellulose nanofiber.[55] PC is known for its superior structural integrity and mechanical properties and preferred choice in architectural applications.[56,57] However, despite these advantageous traits, its high melt viscosity, which arises from its rigid chain structure, poses challenges during processing.[58] This difficulty may account for the relatively limited research on its use as a matrix material in 3D printable NFRPCs within the existing literature. Optimizing NFRPC, created by reinforcing PC with hemp—a sustainable and mechanically

15480569, 2025, 8, Downloaded from https://4spepublications.onlinelibrary.wiley.com/doi/10.1002/pc.29460 by Turkey Cochrane Evidence Aid, Wiley Online Library on [06/06/2026]. See the Terms and Conditions (https://onlinelibrary.wiley.com/terms-and-conditions) on Wiley Online Library for rules of use; OA articles are governed by the applicable Creative Commons License

superior fiber—for 3D printing use holds great potential in terms of contributing to literature, expanding architectural usage areas, and promoting sustainability.

In the FDM process, a 3D design is created with computer-aided design (CAD) software and then imported into a slicer program to define the printing parameters. The parameters are saved in the STereo Lithography interface (STL) format and transferred to the 3D printer. During printing, the thermoplastic filament is continuously fed into a heated chamber where it undergoes a phase change, transforming into a highly viscous fluid. This molten material is then through a nozzle and systematically deposited layer by layer onto a heated table.[37] The ease of processing in the 3D printer and the quality of prints obtained are influenced by the lower melting (T_m) and glass transition temperatures (T_g) of the filament.[59] PC, known for its high T_g value, can have its processing windows widened by reducing its T_g value. According to Jiang et al. (2014), one effective and simple method to achieve this, especially for amorphous polymers like PC, is by adding a plasticizer.[60] Past studies indicate that plasticizers, which also function as flame retardants in polycarbonate (PC), commonly utilize bromoaromatic additives.[61] However, due to increasing environmental concerns and issues related to end-of-life disposal, there is a growing interest in halogen-free alternatives. Following the restrictions on several brominated flame retardants (BFRs), phosphorus-based systems have become frequently suggested substitutes.[62] Aryl phosphates are recognized as effective halogen-free plasticizers for PC blends, praised for their thermal stability and compatibility with various polymers.[63,64] These aryl phosphates include monophosphates like triphenyl phosphate (TPP) and bisphosphates such as resorcinol bis(diphenyl phosphate) (RDP).[64] Regarding TPP, its low water solubility and relatively high soil adsorption coefficient lead to rapid adsorption onto sediments in rivers and ponds. Its biodegradation in aquatic environments occurs swiftly. There have been no reported cases of neurological diseases among workers in TPP manufacturing plants, nor have there been instances of delayed neurotoxicity from TPP poisoning, indicating that it poses minimal risk to health and the environment.[65] Given that the primary focus of this study is to enhance sustainability by mitigating environmental harm, the benefits of utilizing TPP as a plasticizer in PC composites are clearly significant.

It is known that the mechanical, flame retardant, biodegradable, thermal, and physical properties of polymer composites can be significantly influenced by the incorporation of plasticizers.[66] Jung et al. (1998) observed that when TPP, a plasticizer with flame retardancy, was added to the PC/ABS composite, T_g and thermal degradation values decreased, while tensile strength and LOI values increased.[67] Lei and Chen (2008) added di-n-dodecyl phosphate and TPP plasticizers to the PBT/PC composite. The addition of TPP resulted in a greater decrease in T_g than the addition of di-n-dodecyl phosphate.[68] Feyz et al. (2010) added TPP to the PC/ABS composite and observed that viscose parameters increased.[69] Jang et al. (2005) added TPP and RDP to PC and the thermal strengths of both flame-retardant plasticizer additions were almost the same.[64] Swoboda et al. (2008) observed an increase in flexural modulus value and a decrease in thermal strength when TPP was added to PETG/PC composite. In addition, SEM images of the composite obtained by adding TPP to PC showed a more homogeneous structure compared to PETG/TPP.[70] Furthermore, plasticizers are known to improve interfacial interaction between fiber and matrix material for NFRPC, as well as affecting mechanical, chemical, thermal, etc. properties.[71] These findings indicate that the addition of plasticizers, particularly TPP, may confer various advantages to hemp fiber-reinforced PC composites, potentially impacting mechanical, chemical, and morphological properties.

FDM is widely researched due to its numerous advantages. Furthermore, this technique enables the utilization of conventional thermoplastic polymers as well as composite materials.[72] However, to the best of the authors' knowledge, there are currently no studies in the literature focused on optimizing TPP-added hemp fiber-reinforced polycarbonate for the FDM technique and 3D printers. This study has evaluated the effects of TPP on hemp fiber-reinforced polycarbonate composites. The goal was to improve the flow and processing characteristics of these composites for 3D printing, thereby expanding their potential applications in architecture by enhancing their mechanical, morphological, flame retardancy, and rheological properties. The study examined three different TPP ratios: 5%, 10%, and 20%. The TPP-added samples were compared against both hemp fiber-reinforced polycarbonate and pure polycarbonate. A constant melt-mixing temperature and printing nozzle temperature were maintained for all samples to assess viscosity. Characterization of the composites was conducted using Fourier-transform infrared spectroscopy (FTIR), thermogravimetric analysis (TGA), differential scanning calorimetry (DSC), rheological analysis, tensile testing, limiting oxygen index (LOI), and scanning electron microscopy (SEM) analyses.

2 | EXPERIMENTAL

2.1 | Materials

The control sample used was pure PC. The matrix material, suitable for general use, was provided by Lotte

15480569, 2025, 8, Downloaded from https://4spepublications.onlinelibrary.wiley.com/doi/10.1002/pc.29460 by Turkey Cochrane Evidence Aid, Wiley Online Library on [06/06/2026]. See the Terms and Conditions (https://onlinelibrary.wiley.com/terms-and-conditions) on Wiley Online Library for rules of use; OA articles are governed by the applicable Creative Commons License

TABLE 1 Composition ratio, mixing speed, melt-mixing temperature, and mixing times of composite samples.

Sample	Composition (%)	Mixing speed (rpm)	Mixing temperature (°C)	Mixing time (min)
PC	PC: 100	100	250	4
PCH	Hemp/PC: 10/90	100	230	4
PCH5T	(Hemp/PC: 10/90) **95**/TPP **5**	100	230	4
PCH10T	(Hemp/PC: 10/90) **90**/TPP **10**	100	230	4
PCH20T	(Hemp/PC: 10/90) **80**/TPP **20**	100	230	4

Notes: The information highlighted in bold indicates the quantity of the TPP fillers in relation to the Hemp/PC matrix within the composites.
Abbreviations: Hemp, alkali-treated hemp fibers; PC, polycarbonate; TPP, triphenyl phosphate.

Chemical, Seul, South Korea, with a specific gravity of 1.20, tensile strength: 63–70 MPa, impact strength: 80–85 kJ/m^2, vicat softening and deformation temperatures are: 150°C and 130°C, and melt fluidity index of 10. The hemp fibers, supplied by Hemp Traders Los Angeles, America, were used in raw state, degummed, and had the lignin left intact. The fibers were uniformly aligned. Sodium hydroxide (NaOH) at 99% purity was obtained from Katki Dunyasi, Turkey. TPP, also known as phosphoric acid triphenyl ester, with a molar mass of 326.29 g/mol, melting range of ≤50°C, and density of 1.2 g/cm^3 at 50°C, was supplied from Merck, Darmstadt, Germany.

2.2 | Composite filament preparation

Firstly, hemp fibers were cut into 6 mm lengths, followed by treatment with a 5% NaOH/pure water solution. This mixture was then stirred at 120°C for 60 minutes at 200 rpm using an MSH-20D Digital Heating Magnetic Stirrer from (DAIHAN SCIENTIFIC, South Korea). Subsequently, the fibers were washed with tap water to eliminate the solution and neutralize it. After washing, the fibers were air-dried overnight at ambient temperature. Following this, the dried hemp fibers and PC granules underwent dehumidification in a Witeg oven at a temperature of 80°C and a pressure of −0.6 bar for 24 h. The dehumidified PC and hemp fibers were then separated to create composite filaments. Within the scope of the study, five different filaments were produced. The first filament consisted of a neat PC and was utilized as a reference sample. The second sample comprised hemp fiber-reinforced PC with a 10/90 fiber/matrix ratio. This ratio was selected based on the findings of our previous study, where the most favorable mechanical, chemical, thermal, and morphological properties for hemp fiber/PC composite were obtained with 10% hemp fiber compared to different ratios.[73] Additionally, three different ratios were determined for the composite samples containing TPP. In these composites, the hemp fiber/PC ratio was fixed at 10/90, and TPP was added to the mixture at 5%, 10%, and 20%, respectively. The materials were then fed into the twin-screw extruder (DSM Xplore 15 cc Micro-compounder, Netherlands) through the feed hopper. They were then blended at specified ratios, speed, and melt-mixing temperature as detailed in Table 1. PC pellets were added first and mixed for 4 min, while hemp fibers and TPP were added during the last minute of mixing. After a total mixing time of 4 min, the composite material was extruded from the nozzle of the extruder device and shaped into filament form with the help of a conveyor belt. The resulting filaments had diameters of 1.0–2.0 mm, making them suitable for use in a 3D printer. The pure PC composite maintained a transparent appearance, which is characteristic of the material itself. However, the addition of hemp fiber resulted in yellowish-brown filaments with color transitions due to its natural content (see Figure 1.). The addition of TPP did not result in any discernible visual changes.

2.3 | 3D-Printed composites

The Anycubic 13 3D printer (made in China) was selected for the implementation of the FDM process in this study. To begin the process, an STL file was created from a 3D CAD model. Subsequently, the slicer software was used to generate G-code tailored to the specific 3D printing parameters specific to the 3D printer.[74] The 3D CAD models were created using the Rhinoceros program. In Rhinoceros, models measuring 75 × 12 × 2 mm and 130 × 6.5 × 3.2 mm were designed for the tensile test, LOI, and UL94 tests, and exported in STL format. Each file was then imported into the slicer software Ultimaker Cura, where the specified parameters from Table 2. were input. The models with the designated parameters were sliced, saved in G-code format, and transferred to the printing device. Once the files were uploaded to the device, the prepared composite filaments

15480569, 2025, 8, Downloaded from https://4spepublications.onlinelibrary.wiley.com/doi/10.1002/pc.29460 by Turkey Cochrane Evidence Aid, Wiley Online Library on [06/06/2026]. See the Terms and Conditions (https://onlinelibrary.wiley.com/terms-and-conditions) on Wiley Online Library for rules of use; OA articles are governed by the applicable Creative Commons License

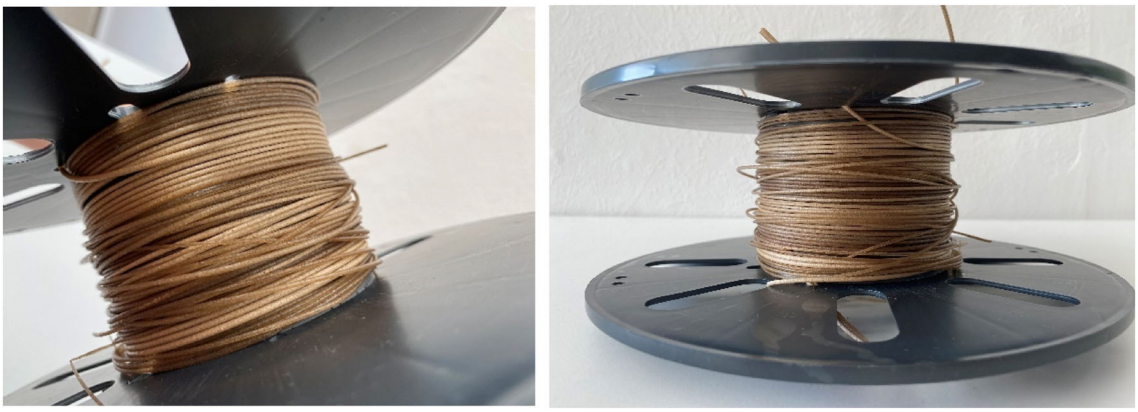


FIGURE 1 (A, B) Hemp fiber-reinforced polycarbonate composite filaments.

TABLE 2 3D printing parameters.

3D Printing parameters	
Height of the first layer (mm)	0.3
Height of the layers (mm)	0.1
Width of the layer (mm)	0.4
Filling pattern	Line
Filling ratio (%)	100
Filling alignment (degree, angle)	45
Thickness of shells (mm)	1.0
Count of shells	2
Print speed (mm/s)	45.0
Nozzle diameter (mm)	1.0
Printing temperature (°C)	245
Printing bed temperature (°C)	110

were fed into the filament feeding unit of the 3D printing device, and the AM process commenced. For the tensile test, LOI, and UL94 V tests, the number of printing layers was 18, 30, and 30, respectively. The PC, PCH, PCH5T, PCH10T, and PCH20T filaments were printed in triplicate for each test method. All samples were printed at the same temperature to observe their flowability. In the initial stage, it was observed that compared to pure PC, the samples with added TPP flowed and were processed more easily. This will be further elucidated by the T_g values obtained from DSC analysis.

2.4 | Characterization

The FTIR spectra measurements conducted in this study were carried out using the Spectrum IR program with a wavelength of 4000–650 cm^{-1} on a Spectrum 100 FTIR device with an ATR unit (Perkin Elmer, USA). The analysis was repeated twice to ensure the accuracy of the data.

Thermogravimetric analysis (TGA) is used to measure the mass changes of materials in response to enhancing temperatures or over time. In this study, TGA was conducted using the MTTA18110856 TGA 1 (Mettler Toledo, Turkey) device. The TGA analysis was conducted over a temperature range from 25°C to 600°C, using a heating rate of 10°C/min and a nitrogen flow rate of 30 mL/min. The analysis was repeated twice to ensure the accuracy of the data.

DSC is a thermal analysis method that examines the variation of a material's heat capacity as temperature changes. The DSC analysis was conducted using nitrogen gas and a Mettler Toledo DSC 1 (Mettler Toledo, Turkey) machine. A two-stage analysis was employed, with a temperature increase of 10°C/min between 25°C and 250°C. In the initial heating stage, the thermal traces from the twin-screw extruder were eradicated, and the results from the subsequent heating stage were examined to determine the T_g values of the samples. This analysis was performed twice to confirm the reliability of the data.

The rheological properties were examined using a stress-controlled oscillatory-rotational rheometer with parallel plates (Anton Paar MCR 102, Austria) at a temperature of 230°C. Frequency sweep tests were performed across a frequency range of 0.1–628 rad/s, maintaining a constant strain of 1%. his assessment provided data on complex viscosity (η^*), along with the storage modulus (G') and loss modulus (G''). The analysis was repeated twice to ensure the accuracy of the data.

In the tensile test, the tensile strength values which signify the maximum force a material can withstand before breaking or fracturing were examined. Tensile strength holds great significance in architectural

15480569, 2025, 8, Downloaded from https://4spepublications.onlinelibrary.wiley.com/doi/10.1002/pc.29460 by Turkey Cochrane Evidence Aid, Wiley Online Library on [06/06/2026]. See the Terms and Conditions (https://onlinelibrary.wiley.com/terms-and-conditions) on Wiley Online Library for rules of use; OA articles are governed by the applicable Creative Commons License

applications. The study involved subjecting five 75 × 12 × 2 mm bars from each composite specimen to a tensile test. Composite specimens were evaluated using an Instron Tensile Machine Model 3345, USA, applying the Instron Bluehill Universal software and following the ISO 527-5A standard at a speed of 10 mm/min.[75] A minimum of five samples were subjected to tensile tests to ensure data accuracy.

The electron microscope (SEM, Quanta FEG 450, Taiwan) was utilized to analyze the morphology of composite samples. The device operated in secondary electron mode at a current of 15.00 kV and a pressure of 4.48e-4 Pa utilizing zoom ratios of 100, 500, and 1000. The samples analyzed were sourced from tensile tests conducted on composite materials produced with the 3D printer. Given that the samples are composed of insulating materials, they underwent a coating process to enhance their conductivity. The gold plating was applied for a duration of 90 s to achieve the required conductivity under a current voltage of 10 mA.

The flame resistance of samples was assessed using the LOI test. which determines the minimum concentration of oxygen needed to sustain candle-like combustion in plastics. LOI values were obtained with an oxygen meter (M-LOI-01) from Mares Analysis Instrument Factory, Turkey, utilizing specimens with dimensions of 80 × 10 × 4 mm^3 following TS EN ISO 4589-2.[76] The LOI tests were applied to at least five samples to ensure the accuracy of the data.

Additionally, UL-94 vertical burning tests were conducted using samples measuring 130 × 6.5 × 3.2 mm^3, following the ASTM D-635[77] standard with an M-LOI-01 device from Mares Analysis Instrument Factory, Turkey. In this test, the samples were positioned vertically above a cotton patch, and the ratings were determined based on the American National Standard UL-94.

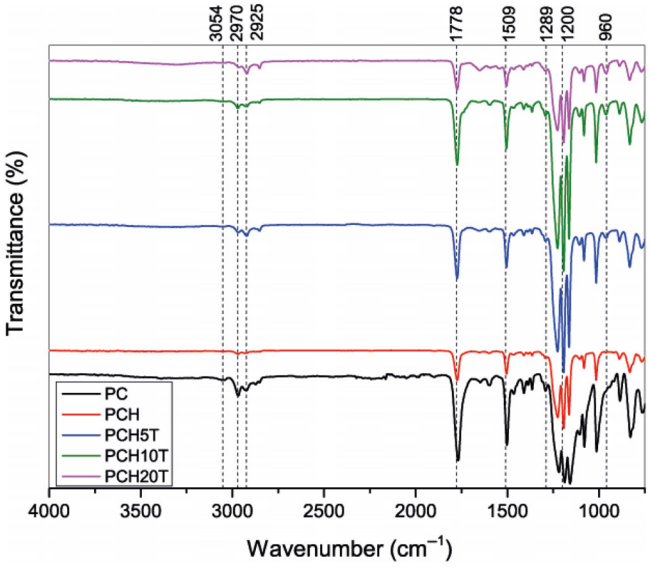


FIGURE 2 FTIR spectra were obtained from the composites.

3 | RESULTS AND DISCUSSION

3.1 | FTIR

The FTIR spectra of the composite samples are shown in Figure 2. Besides, the comparison of the chemical groups observed in the samples coded PC, PCH, PCH5T, PCH10T, and PCH20T is presented comparatively in Table 3. According to Jang ve Wilkie (2005), 960 and 1200 cm^{-1} bands correspond to the phosphorus–oxygen double bond stretching (P═O) and phosphorus–oxygen-single bond stretching (P—O). Since the P—O stretching band overlaps with the carbon–oxygen stretching region (1150–1300 cm^{-1}) of polycarbonate compounds, the band at 960 cm^{-1} is used as the diagnostic band for phosphates.[64] Upon analyzing the 960 cm^{-1} band, no peak is observed in the PCH sample, whereas dominant peaks are present in the PCH5T, PCH10T, and PCH20T

TABLE 3 FTIR spectra of the composites.

Wave number (cm^{-1})	Associated chemical groups	PC	PCH	PCH5T	PCH10T	PCH20T
960	P—O single bond stretching	None	None	Low	Low	Low
1200	P═O double bond stretching	High	High	Dominant	Dominant	Dominant
1289	C—H bending	Low	Very low	Low	Low	Low
1509	Aromatic C—H	Dominant	Low	High	High	Low
1778	C═O stretching	Dominant	Low	High	Dominant	Low
2925	α-Cellulose	Low	Very low	Low	Low	Low
2970	Methylene group	High	Very low	Low	Low	Low
3054	C—H stretching	Low	None	Very low	Very low	Very low

15480569, 2025, 8, Downloaded from https://4spepublications.onlinelibrary.wiley.com/doi/10.1002/pc.29460 by Turkey Cochrane Evidence Aid, Wiley Online Library on [06/06/2026]. See the Terms and Conditions (https://onlinelibrary.wiley.com/terms-and-conditions) on Wiley Online Library for rules of use; OA articles are governed by the applicable Creative Commons License

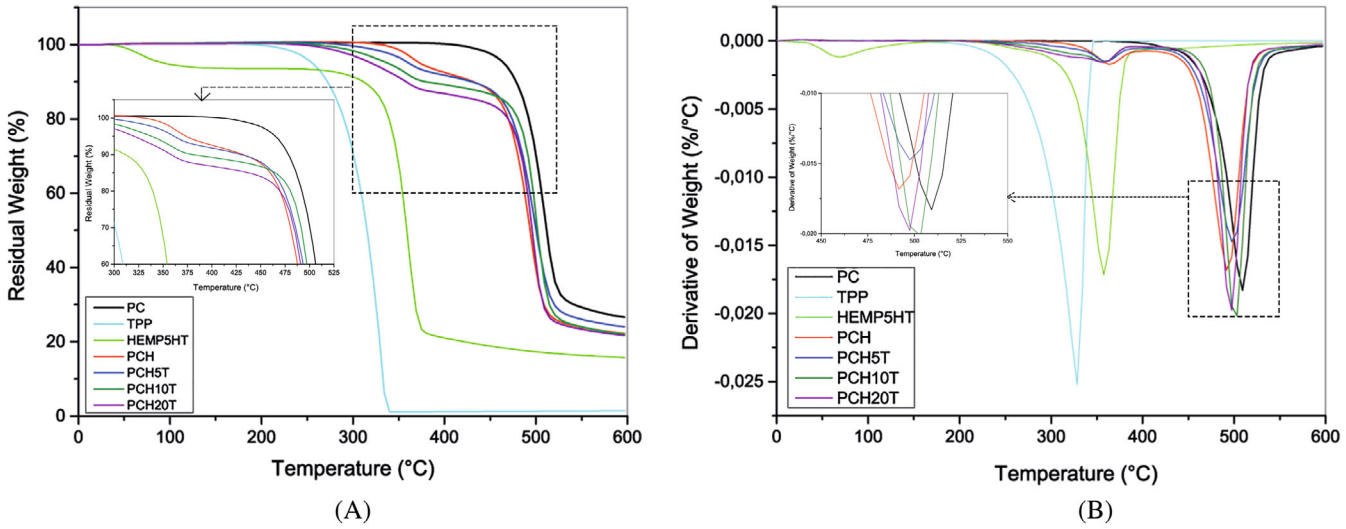


FIGURE 3 TGA (A) and DTG (B) thermograms of composites.

samples. This peak is attributed to the phosphate content of TPP. The 1778 cm^{-1} C═O stretching vibration is known as the carbonate characteristic band, and the 1509 cm^{-1} band is associated with aromatic C—H.[78–80] Upon examining the 1778 cm^{-1} band, the most prominent peak is observed in the PCH10T sample after pure PC. Additionally, the vibration intensity between 1778 and 1509 cm^{-1} wavelengths is predominant in pure PC and TPP-added samples, with the PCH10T sample showing the most dominant peaks among TPP-added samples. This indicates a higher preservation of carbonate linkage structures in the PCH10T sample, which in turn enhances the flame retardancy of PC. As noted by Apaydin Varol et al. (2014), the peak in the range of 2870–3054 cm^{-1} is associated with C-H stretching, while the range of 1278–1326 cm^{-1} corresponds to C—H bending.[81] Methyl groups are present at wavelengths of 2850–3000 cm^{-1},[82] and these peaks are predominantly observed in the pure PC sample, with almost no presence in the fiber-added PCH sample. Additionally, peaks resulting from TPP addition to the composite are noted.

3.2 | TGA analysis

The TGA and derivative weight (DTG) curves of the composite samples are depicted in Figure 3, and the heat-induced mass loss values are presented in Table 4. Based on the data from the table, pure PC exhibits a single-stage degradation, while the composites undergo degradation in two stages. The TGA analysis reveals that the temperatures at which the hemp fiber-reinforced PC composite experiences 5% and 10% weight loss decrease as the amount of TPP increases. This decrease can be linked to the low thermal strength of TPP. Additionally, the addition of TPP to the composite enhances thermal stability at high temperatures, as evidenced by the temperatures at which 50% weight loss occurs. Notably, the PCH10T sample demonstrates superior thermal stability at 50% weight loss temperature, with only a 1.92% reduction compared to pure PC, and approximately 8 degrees increase compared to the TPP-free composite (PCH).

TABLE 4 Mass loss due to heat observed in the TGA analysis of composite filament samples.

Sample	5% Weight loss temperature (°C)	10% Weight loss temperature (°C)	50% Weight loss temperature (°C)
TPP	255.67	272.45	315.23
HEMP5HT	94.20	311.01	358.84
PC	465.37	478.37	511.51
PCH	373.10	431.40	493.47
PCH5T	361.36	429.30	500.18
PCH10T	337.45	379.81	501.86
PCH20T	319.84	357.59	495.99

In Table 5, the onset (T_{onset}) and maximum degradation (T_{max}) temperatures, as well as char residue values, are presented. T_{onset} represents the temperature at which 5% weight loss occurs in TGA curves, while T_{max} corresponds to the peaks in DTG curves. Polycarbonate (PC) exhibits high thermal stability, initiating degradation at high temperatures ($T_{onset} = 485.52$) with a high T_{max}. However, adding hemp fiber to PC results in decreased T_{onset} and T_{max} values. Conversely, the incorporation of TPP into the PCH composite enhances its

15480569, 2025, 8, Downloaded from https://4spepublications.onlinelibrary.wiley.com/doi/10.1002/pc.29460 by Turkey Cochrane Evidence Aid, Wiley Online Library on [06/06/2026]. See the Terms and Conditions (https://onlinelibrary.wiley.com/terms-and-conditions) on Wiley Online Library for rules of use; OA articles are governed by the applicable Creative Commons License

TABLE 5 T_{onset}, T_{max}, and char residue of composite samples.

Samples	T_{onset} (°C)	T_{max} (°C)	Char residue at 600°C
PC	485.52	508.57	26.52
TPP	305.01	328.65	1.42
HEMP5HT	340.48	359,68	15.73
PCH	463.27	493.47	22.21
PCH5T	468.78	498.09	23.93
PCH10T	471.60	501.44	22.02
PCH20T	467.73	496.41	21.66

thermal strength, leading to a higher maximum degradation temperature. This aligns with findings from existing literature. The presence of phosphorus in the sample influences the makeup of intermediate chars during the second stage of thermal degradation, leading to a reduction in reaction rates within the decomposed residue.[83] Furthermore, previous research by Jang et al. suggests that phosphate can stabilize carbonate linkage from oxidative degradation in TGA.[64] This is further supported by FTIR results, showing that the carbonate linkage is highest at 10% TPP and is like PC. Notably, the PCH10T sample demonstrates the highest value, with the maximum degradation temperature closely resembling that of PC. This mirrors the behavior observed with the addition of S-BDP, a phosphorus-based flame-retardant plasticizer, to PC.[78] Additionally, the addition of TPP results in minimal change in the char residues compared to the PCH composite, indicating that TPP does not significantly impact the char-forming ability of the composites. In literature, Shao et al. also discovered that adding TPP to PC had no impact on the char-forming capability of the composites.[84]

3.3 | DSC analysis

The DSC results for the composites are presented in Table 6. There was no notable change in the T_g value of the PCH composite sample consisting of hemp fiber added to pure PC. This finding is consistent with a similar study on hemp-strengthened PLA as reported in the literature.[85] Analysis of the T_g values obtained from the DSC analysis indicated a general reduction in T_g values with the addition of TPP to the composite. It is known from the literature that TPP has a plasticizing effect on PLA.[86] Swoboda et al. also discovered a decrease in viscosity and plasticization effect with the addition of TPP to PC in their study,[70] like the effect observed with

TABLE 6 DSC analysis results of the composite samples.

Sample	T_g (°C)	
	1st Stage	2nd Stage
PC	150.13	148.44
PCH	150.11	148.99
PCH5T	136.18	136.05
PCH10T	119.33	120.31
PCH20T	89.90	93.74

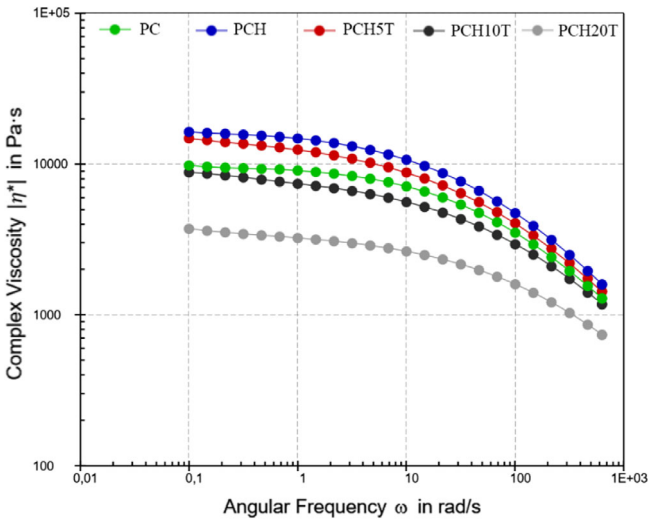


FIGURE 4 Complex viscosity of pure PC, PCH, PCH5T, PCH10T, and PCH20T samples.

the PCH sample. The increased plasticity is evident from the improved flow of the composite material from the nozzle, making it more fluid and easier to process using the 3D printer.[73] The presence of a plasticizing effect is reflected in the decrease in T_g with increasing TPP ratio. Consequently, the addition of TPP to the composite resulted in a material that can be more easily processed in a 3D printer.

3.4 | Rheological properties

To determine the viscosity and modulus parameters of the composite samples, sweep frequency rheological analysis was performed. The complex viscosity (η^*), storage (G'), and loss (G'') modulus curves of pure PC, PCH, PCH5T, PCH10T, and PCH20T samples versus angular frequency are shown in Figure 4. According to Figure 4, only the pure PC exhibited a complete Newtonian behavior between 0.1 and 1 rad/s. The addition of 10% hemp fiber increased the viscosity value of pure PC. With the

15480569, 2025, 8, Downloaded from https://4spepublications.onlinelibrary.wiley.com/doi/10.1002/pc.29460 by Turkey Cochrane Evidence Aid, Wiley Online Library on [06/06/2026]. See the Terms and Conditions (https://onlinelibrary.wiley.com/terms-and-conditions) on Wiley Online Library for rules of use; OA articles are governed by the applicable Creative Commons License

addition of TPP, the viscosity value started to decrease. It is seen that when the TPP ratio is more than 10%, the fluidity of the composite will be easier than pure PC. This coincides with the laboratory observation that composite samples with high TPP ratios are easier to print on a 3D printer than pure PC and PC composite samples containing only hemp fiber. Twite-Kabamba et al. (2009) observed similar findings in their research on hemp fiber-reinforced PP composite. The addition of hemp fiber enhanced complex viscosity values. However, the introduction of a compatibilizer to the hemp fiber-reinforced PP composite had a plasticizing effect, leading to a decrease in viscosity values.[87] Jang (2018) observed that reinforcing the PC matrix with natural fiber increased complex viscosity.[88] It is also known from the literature that adding plasticizers to PC lowered viscosity and improved melt flow.[89]

The storage modulus represents the capacity to store energy imparted by external forces, and it exhibited an increase in angular frequency across the entire range of applied frequencies.[90] The relation between the storage modulus and the angular frequency of the composite samples is illustrated in Figure 5A. The storage modulus of PC significantly increased with the addition of hemp fiber. This is mainly due to the enhanced stiffness of the matrix resulting from the reinforcing effect of the natural fiber as mentioned in the literature.[91] It is also known that the storage modulus value increases because of adding hemp fiber to PLA.[72] The loss modulus is a measure of the permanent structural change or energy dissipation within a material caused by applied stress. The relationship between the loss modulus and the angular frequency of the composite samples is illustrated in Figure 5B. It was observed that when hemp fiber was added, the loss modulus value of pure PC increased, while it decreased with the addition of TPP. The rise in loss modulus with the incorporation of hemp fiber aligns with existing literature.[27] Generally, adding TPP reduces the viscosity and facilitates its processability in 3D printers.

3.5 | Mechanical characteristics

To determine the mechanical properties, specimens were printed on the Anycubic I3 Mega 3D printer following the test standard. Tensile tests were performed at least five times for each sample and compared with 3D-printed pure PC. Figure 6 shows the specimens printed for tensile testing and the fractured specimens resulting from the tests. The fracture point of the pure PC sample appears smooth, whereas the fracture point of the composites, which contain hemp fibers and/or TPP, appears more jagged. The reason for this is thought to be the bridging action of the fibers at the moment of fracture. Reviewing the tensile test results in Table 7, it is evident that the maximum tensile strength of the PCH sample reinforced with hemp fiber increased by 11.9% compared to pure PC. In the literature, it is noted that the tensile strength value increases when the PC is reinforced with natural fiber.[92] Additionally, an increase in tensile strength was observed in direct proportion to the TPP added to the composites. Compared to pure PC, PCH5T, PCH10T, and PCH20T samples showed increases of 23.5%, 33.1%, and 37.8%, respectively. PCH10T composite showed an increase of 18.93% compared to PCH composite without TPP. According to existing literature, the addition of phosphorus-based plasticizers to PC[93]

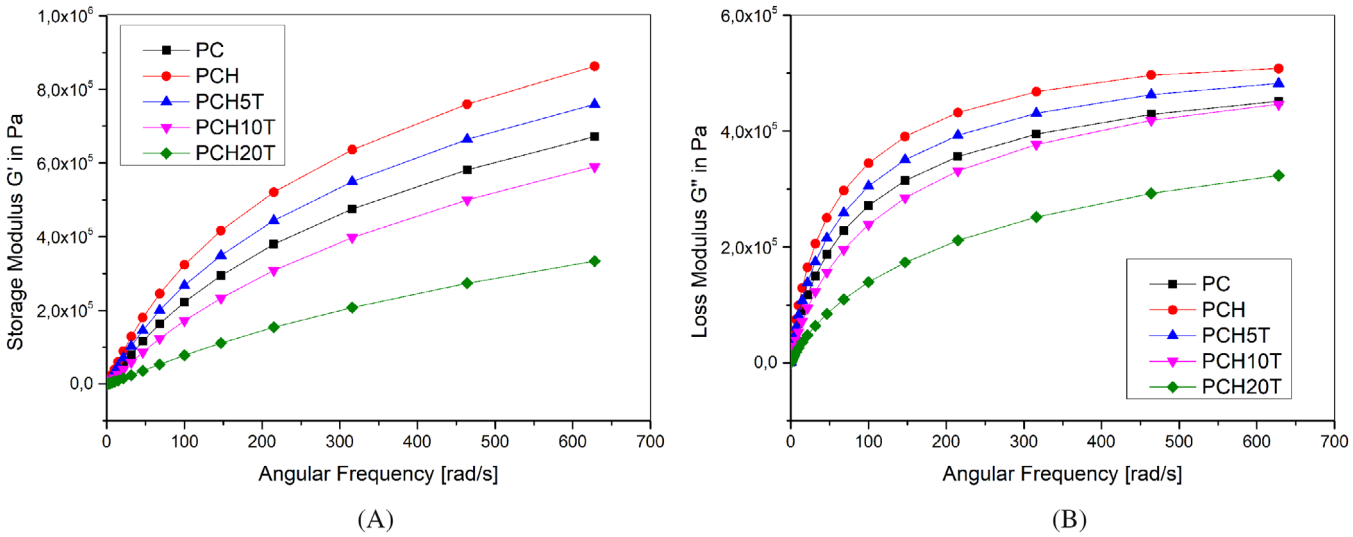


FIGURE 5 (A) Curves of storage modulus as a function of frequency. (B) Curves of loss modulus as a function of frequency for the composite samples.

15480569, 2025, 8, Downloaded from https://4spepublications.onlinelibrary.wiley.com/doi/10.1002/pc.29460 by Turkey Cochrane Evidence Aid, Wiley Online Library on [06/06/2026]. See the Terms and Conditions (https://onlinelibrary.wiley.com/terms-and-conditions) on Wiley Online Library for rules of use; OA articles are governed by the applicable Creative Commons License

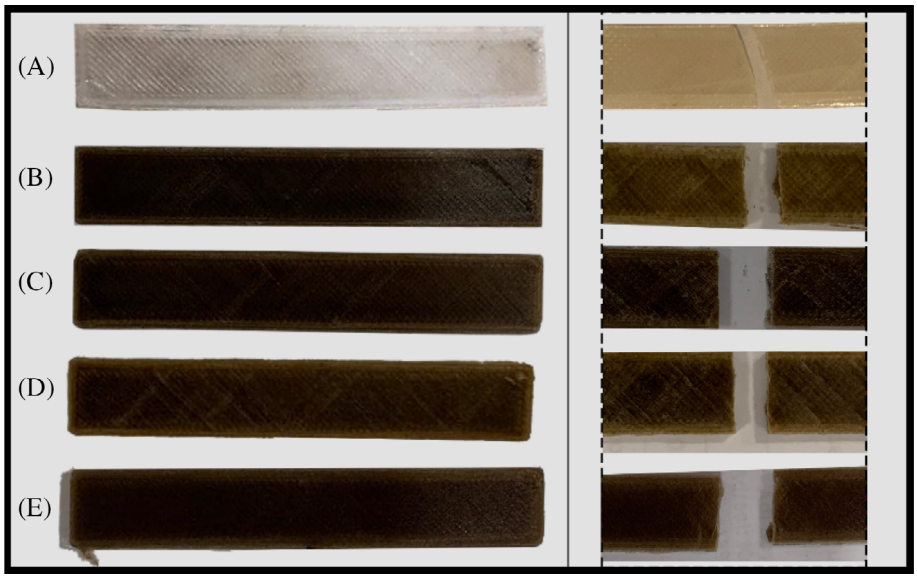


FIGURE 6 3D-printed composite specimens obtained before tensile testing on the left and after tensile testing on the right. (A) pure PC; (B) PCH; (C) PCH5T; (D) PCH10T; (E) PCH20T.

TABLE 7 Tensile strength of the composites.

Sample	Tensile stress at maximum force (MPa)	Young's modulus (MPa)	Tensile strain at maximum force (%)
PC	43.19 ± 0.98	2543.35 ± 130	4.78 ± 0.08
PCH	48.34 ± 0.38	3271.34 ± 80.8	5.74 ± 0.10
PCH5T	53.34 ± 1.23	3517.70 ± 110	5.77 ± 0.86
PCH10T	57.49 ± 1.93	3923.56 ± 68.4	5.79 ± 0.75
PCH20T	59.52 ± 1.61	4924.16 ± 83.3	6.27 ± 0.17

and TPP to PC/PETG blend[70] leads to increased mechanical properties. The reason why this situation is similar in PCH5T, PCH10T, and PCH20T composites is thought to be that TPP provides a more rigid structure by filling the gaps between the fiber matrix. The tensile strain values are presented in Table 7. also indicates that incorporating hemp fiber enhances the toughness value of pure PC. Del Rey et al. (2017) found that the toughness of a polypropylene matrix was also improved when reinforced with hemp fiber.[94] Consequently, the increase in toughness within the polycarbonate matrix due to hemp fiber aligns with existing literature. The incorporation of TPP, a plasticizer, into the composite results in a notable enhancement of the toughness values. A review of existing literature indicates that comparable outcomes have been observed when plasticizers are integrated into polycarbonate (PC) materials.[89]

3.6 | SEM analysis

The SEM images captured from the fractured surfaces during the tensile testing of 3D printed pure PC are presented in Figure 7. A porous structure is observed on the surface. The reason for this structure is known to be due to the FDM technique.[95]

SEM images taken from the fractured surfaces of the 3D-printed PCH, PCH5T, PCH10T, and PCH20T tensile tests were displayed in Figure 8. Compared to the PCH sample, it is observed that the gaps around the fibers in the PCH5T, PCH10T, and PCH20T samples, to which TPP was added, have decreased. As the TPP ratio increases, the voids between the hemp fiber and the polycarbonate matrix diminish, resulting in a more consolidated and rigid structure. This observation aligns with the findings in the study by Menčík et al., where a decrease in voids was noted upon the addition of a plasticizer to 3D-printed PHB/PLA.[66] It seems that TPP is effectively dispersed in the composite material, contributing to the interfacial interaction. The rigid micro-scale structure accounts for the observed increase in mechanical properties. Furthermore, it is well-documented that the dispersion of flame-retardant plasticizers within a polymer greatly influences their flame retardancy performance.[96] Considering this, whether the mechanical properties enhanced by well-dispersed TPP exhibit similar improvements in flame-retardant performance through LOI and UL94 V tests have been evaluated.

The SEM image in Figure 9 reveals the micro-scale relationship of the fibrous structure in the composites. In Figure 7A, the PCH composite displays gaps and rough structures on the fiber surfaces. However, in Figure 7B–D, which depicts TPP-added composites, the fiber surfaces appear more filled and smooth previous studies have established that TPP can transform the hollow structure in kapok fiber into a filled cylindrical structure,[97] and it has shown a similar filling effect

15480569, 2025, 8, Downloaded from https://4spepublications.onlinelibrary.wiley.com/doi/10.1002/pc.29460 by Turkey Cochrane Evidence Aid, Wiley Online Library on [06/06/2026]. See the Terms and Conditions (https://onlinelibrary.wiley.com/terms-and-conditions) on Wiley Online Library for rules of use; OA articles are governed by the applicable Creative Commons License

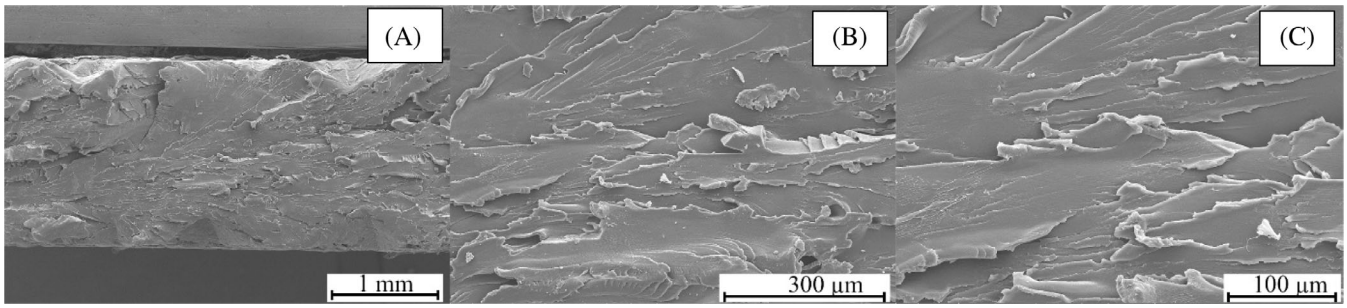


FIGURE 7 SEM images of 3D printed pure PC. (A) ×100; (B) ×500, and (C) ×1000.

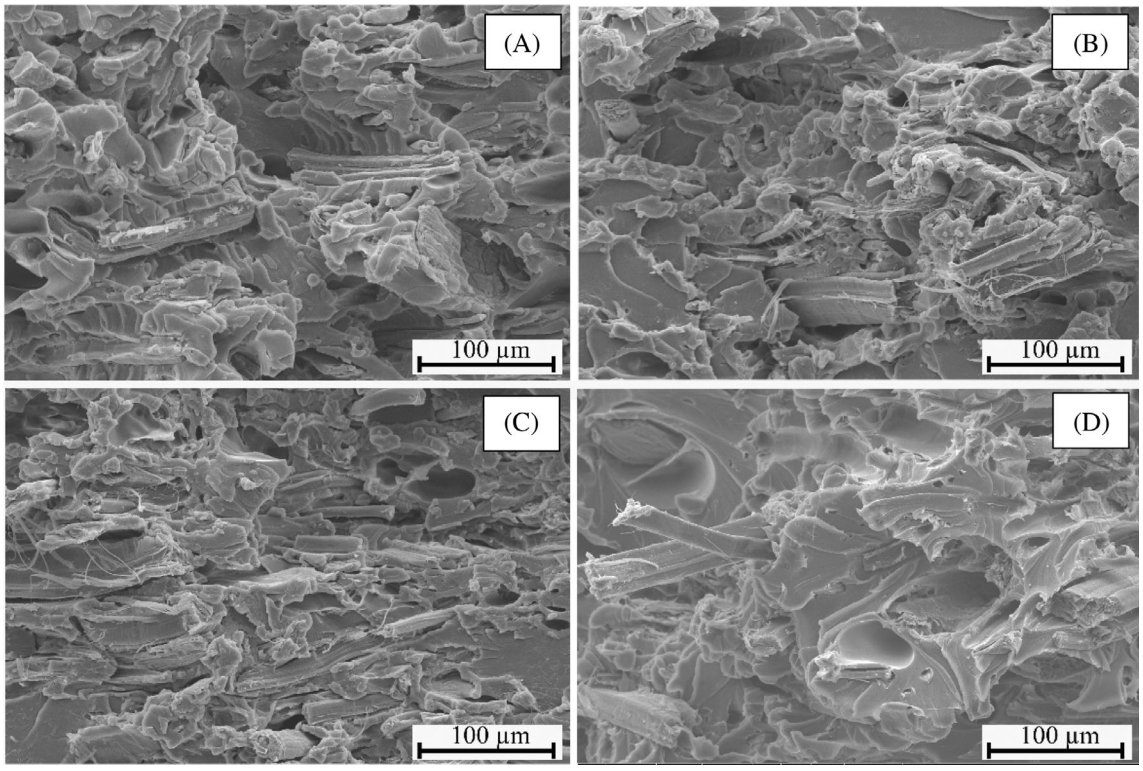


FIGURE 8 SEM images of 3D printed (A) PCH; (B) PCH5T; (C) PCH10T, and (D) PCH20T with a ×1000 zoom ratio.

between hemp fibers and PC matrix. In addition, no interlayer voids were encountered due to the FDM process. Although it is reported that triangle-shaped voids are encountered in 3D printed composites such as natural rubber-strengthened PLA,[98] it is seen that this situation is prevented for NFRPCs produced by using optimum printing temperature and parameters.[99]

3.7 | LOI and UL94 V analyses

Polymeric materials' fire resistance is commonly evaluated using methods such as LOI measurements and UL-94 vertical burning tests. The LOI test is widely recognized as an accurate method for evaluating the flammability of plastics, as it determines the minimum oxygen concentration required for continuous burning.[100] The LOI and UL-94 test results for all composite specimens are outlined in Table 8. Notably, the neat PC has an LOI value of 28, along with melt dripping. The addition of 10-wt% hemp fiber resulted in a slight decrease in PC's LOI values, but no melt dripping occurred. Furthermore, LOI values for PCH5T, PCH10T, and PCH20T samples with added TPP increased by 3.4%, 6.2%, and 12% respectively, compared to pure PC.

Upon reviewing the LOI test samples in Figure 10, it is evident that pure PC burns and flows in a sticky manner, whereas the addition of hemp fiber results in charring behavior. The charring of hemp fiber-containing samples reduces the likelihood of flame spread and

15480569, 2025, 8, Downloaded from https://4spepublications.onlinelibrary.wiley.com/doi/10.1002/pc.29460 by Turkey Cochrane Evidence Aid, Wiley Online Library on [06/06/2026]. See the Terms and Conditions (https://onlinelibrary.wiley.com/terms-and-conditions) on Wiley Online Library for rules of use; OA articles are governed by the applicable Creative Commons License

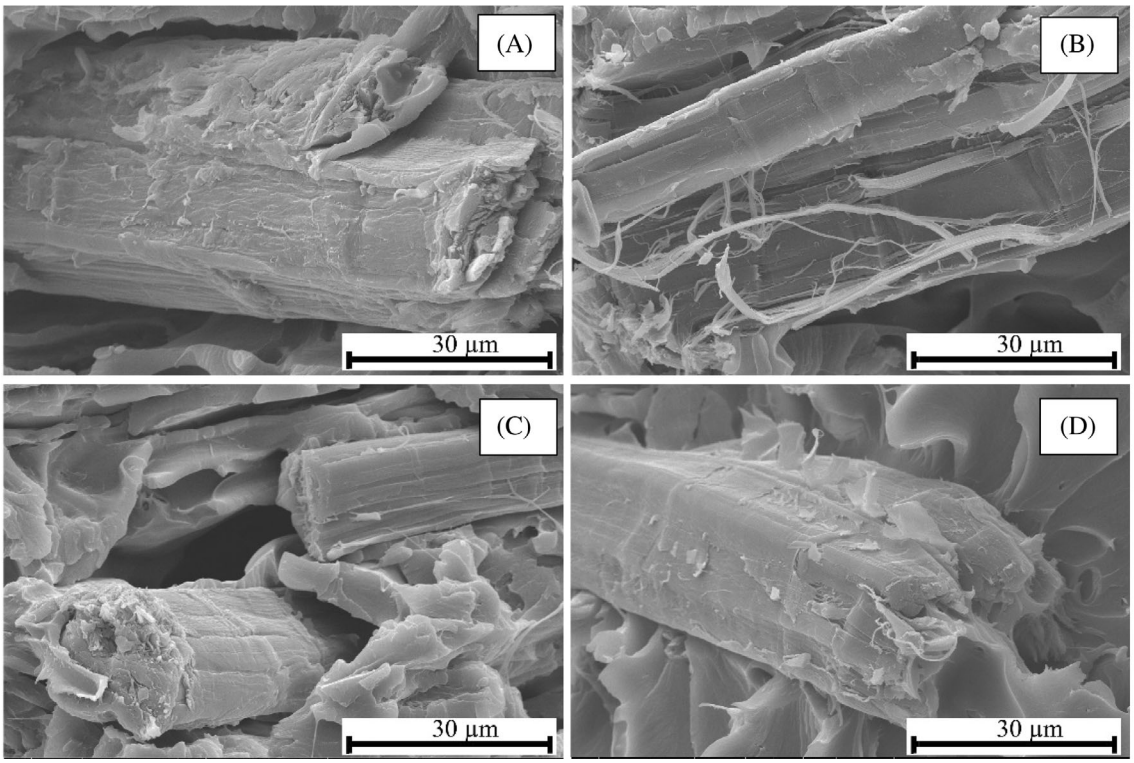


FIGURE 9 SEM images of 3D printed (A) PCH; (B) PCH5T; (C) PCH10T, and (D) PCH20T with a ×5000 zoom ratio.

TABLE 8 LOI and UL-94 test results of neat PC, PCH, PCH5T, PCH10T and PCH20T.

Sample	LOI%O_2	Burning duration (s)	Burning length (if the burning length exceeds the 50-mm limit or not)	UL-94 rating	Dripping
PC	28.9	38	No	V-2	Yes
PCH	28.6	79	No	V-1	No
PCH5T	29.9	115	No	V-1	No
PCH10T	30.7	71	No	V-1	No
PCH20T	32.4	137	No	V-1	No

protects from the ongoing flame, as opposed to pure PC. Shao et al. conducted a vertical combustion test on 10%TPP/PC composite and did not observe a significant expansion of the char crown or a high level of droplet formation.[84] Thus, the char crown observed in the PCH, PCH5T, PCH10T, and PCH20T samples is believed to be derived from the hemp fiber. It is understood that cellulose on the surface is known to break down into char, while hemicellulose beneath the surface decomposes to produce less flammable gases.[83] During the test, outgassing in the form of foam was observed in the TPP-added samples. TPP is known to act as a flame suppressant in the gas phase.[61]

Furthermore, as illustrated in Figure 10, PCH20T generated a more substantial char layer and exhibited prolonged internal burning. The increase in the LOI with the addition of TPP is believed to contribute to this extended burn duration. Supporting this observation, Hazer et al. (2019) reported similar findings when TPP was incorporated into a PLA/PC/GF composite, noting both an increase in the LOI value and a lengthening of the burning duration.[101]

UL-94 test was conducted to determine the flammability of composite samples. The UL-94 results obtained are given in Table 8. While the control sample fell into the V2 category with a burning time of more than 30 seconds and dripping, the hemp fiber-reinforced composite samples with and without TPP fell into the V-1 category with fast extinguishing times. Upon reviewing the literature, Shao et al. (2019) conducted UL94 tests on

15480569, 2025, 8, Downloaded from https://4spepublications.onlinelibrary.wiley.com/doi/10.1002/pc.29460 by Turkey Cochrane Evidence Aid, Wiley Online Library on [06/06/2026]. See the Terms and Conditions (https://onlinelibrary.wiley.com/terms-and-conditions) on Wiley Online Library for rules of use; OA articles are governed by the applicable Creative Commons License



FIGURE 10 Composite samples after LOI tests. (A) pure PC; (B) PCH; (C) PCH5T; (D) PCH10T; (E) PCH20T.

pure PC and PC composites with 10% TPP, yielding comparable results. The test results indicated that pure PC falls within the V-2 category, whereas the PC sample containing 10% TPP has been elevated to the V-1 category.[84] In addition, composite samples prepared by adding TPP at different rates did not drip and the cotton placed under the apparatus from the beginning of the experiment was not ignited by dripping sparks.

4 | CONCLUSION

This article presents a comprehensive analysis of a 3D printable plasticized hemp fiber-reinforced PC composite. The addition of TPP, a plasticizer or flame retardant, plays a pivotal role in altering the characteristics of the material. Various analytical techniques such as FTIR, TGA, DTG, DSC, tensile testing, SEM imaging, LOI, and UL94 V testing were employed to comprehensively understand the behavior and properties of the composite specimens. In FTIR analysis, the band at 960 cm^{-1} was seen as a diagnostic band for the determination of phosphates in TPP added to hemp-reinforced PC composites due to the overlap of the P-O stretching band with the carbon–oxygen stretching region (1150–1300 cm^{-1}) of the polycarbonate matrix. TGA results indicated that the 5% and 10% weight loss temperatures decreased as the TPP content increased. Upon analyzing the DTG curve, it is apparent that the inclusion of hemp fiber in PC results in decreased T_{onset} and T_{max} values. Additionally, the addition of TPP to the PCH composite led to an increase in maximum degradation value being attained at higher temperatures. The DSC analysis revealed that the addition of hemp fiber to the PC matrix did not lead to a significant change in the T_g value. The incorporation of TPP resulted in a progressive decline in the T_g value as the concentration of TPP increased, thereby suggesting the realization of a plasticizing effect. The results of the tensile test indicate that the tensile strength at the maximum force of the PCH specimen increased by 11.9% compared to pure PC. Additionally, a direct relationship was observed between the increase in tensile strength and the TPP ratio added to the composites. Upon reviewing the SEM images, with an increase in TPP content, the gaps between the hemp fiber and the polycarbonate matrix decreased, leading to a more filled and rigid structure. Furthermore, TPP was well dispersed in the composite material, contributing to enhanced interfacial interaction. Upon reviewing the LOI test results, it was seen that the LOI values of TPP-added samples were increased compared to pure PC. Generally, while the pure PC tends to burn and flow in a sticky manner, the samples with added hemp fiber displayed charring behavior. Rheological analysis showed that adding 10% hemp fiber increased the complex viscosity of pure PC, but the addition of TPP significantly reduced it. As a result, thanks to the addition of TPP composite samples are plasticized and ease of flow and process in the 3D printer has been provided. In addition, mechanical, morphological, and flame retardancy properties have been improved compared to pure PC. Thanks to these new advancements, combined with its partial natural content and optimization for 3D printing, it is predicted that it can be an eco-friendly alternative in possible architectural applications to contribute to sustainability.

ACKNOWLEDGMENTS

We thank the Kocaeli University Scientific Research Projects Coordination Unit for supported the project FDK-2022-2923 within the scope of funding doctoral thesis projects.

FUNDING INFORMATION

We thank the Kocaeli University Scientific Research Projects Coordination Unit for funding this study within the scope of 'funding doctoral thesis projects.' Project no: FDK-2022-2923.

15480569, 2025, 8, Downloaded from https://4spepublications.onlinelibrary.wiley.com/doi/10.1002/pc.29460 by Turkey Cochrane Evidence Aid, Wiley Online Library on [06/06/2026]. See the Terms and Conditions (https://onlinelibrary.wiley.com/terms-and-conditions) on Wiley Online Library for rules of use; OA articles are governed by the applicable Creative Commons License

CONFLICT OF INTEREST STATEMENT

The authors are conducting a doctoral thesis within the scope of this study.

DATA AVAILABILITY STATEMENT

This declaration is not applicable.

ORCID

Irem Ceylan Engin https://orcid.org/0000-0003-3761-6004
Nese Cakici Alp https://orcid.org/0000-0002-7626-9212
Ayse Aytac https://orcid.org/0000-0002-9566-7881

REFERENCES

1. Sippach T, Dahy H, Uhlig K, Grisin B, Carosella S, Middendorf P. Structural optimization through biomimetic-inspired material-specific application of plant-based natural fiber-reinforced polymer composites (NFRP) for future sustainable lightweight architecture. *Polymers (Basel)*. 2020;12(12):3048. doi:10.3390/polym12123048
2. Nowotna A, Pietruszka B, Lisowski P. Eco-friendly building materials. *IOP Conf Ser Earth Environ Sci*. 2019;290(1):012024. doi:10.1088/1755-1315/290/1/012024
3. Gholampour A, Ozbakkaloglu T. A review of natural fiber composites: properties, modification and processing techniques, characterization, applications. *J Mater Sci*. 2020;55(3):829-892. doi:10.1007/s10853-019-03990-y
4. Kozlowski R, Wladyka-Przybylak M. *Composites Reinforced with Lignocellulosic Fibers*. Proceedings of the 8th Pacific Rim Bio-Based Composites Symposium; 2006.
5. Kozłowski R, Władyka-Przybylak M. Flammability and Fire Resistance of Composites Reinforced by Natural Fibers. *Polym Advan Technol*. 2008;19(6):446-453. doi:10.1002/pat.1135
6. Naughton A, Fan M, Bregulla J. Fire resistance characterisation of hemp fibre reinforced polyester composites for use in the construction industry. *Compos B: Eng*. 2014;60:546-554. doi:10.1016/j.compositesb.2013.12.014
7. Mohanavel V, Sathish T, Ravichandran M, Ganeshan P, Ravi Kumar MM, Subbiah R. Experimental investigations on mechanical properties of cotton/hemp fiber reinforced epoxy resin hybrid composites. *J Phys Conf Ser*. 2021;2027(1):012015. doi:10.1088/1742-6596/2027/1/012015
8. Behera S, Gautam RK, Mohan S, Chattopadhyay A. Hemp fiber surface modification: its effect on mechanical and tribological properties of hemp fiber reinforced epoxy composites. *Polym Compos*. 2021;42(10):5223-5236. doi:10.1002/pc.26217
9. Arpitha GR, Verma A, Sanjay MR, Siengchin S. Preparation and experimental investigation on mechanical and tribological performance of hemp-glass fiber reinforced laminated composites for lightweight applications. *Adv Civ Eng Mater*. 2021;10(1):427-439. doi:10.1520/ACEM20200187
10. Wang B et al. Flax fibre-reinforced thermoplastic composites. *CSAE*. 2003;57.
11. Li X, Panigrahi S, Tabil LG. A study on flax fiber-reinforced polyethylene biocomposites. *Appl Eng Agric*. 2009;25(4):525-531. doi:10.13031/2013.27454
12. Hu R, Lim JK. Fabrication and mechanical properties of completely biodegradable hemp fiber reinforced polylactic acid composites. *J Compos Mater*. 2007;41(13):1655-1669. doi:10.1177/0021998306069878
13. Ku H, Wang H, Pattarachaiyakoop N, Trada M. A review on the tensile properties of natural fiber reinforced polymer composites. *Compos B: Eng*. 2011;42(4):856-873. doi:10.1016/J.COMPOSITESB.2011.01.010
14. Zafar MF, Siddiqui MA. Effect of filler loading and size on the mechanical and morphological behaviour of natural fibre-reinforced polystyrene composites. *Adv Mater Process Technol*. 2020;7:1-13. doi:10.1080/2374068X.2020.1793261
15. Wirawan R, Zainudin ES, Sapuan SM. Mechanical Properties of Natural Fibre Reinforced PVC Composites: A Review Dissimilar Metal Welding View project Current Progress in Biopolymer-Based Bionanocomposites and Hybrid Materials View project. https://www.researchgate.net/publication/288717510
16. Karsli NG, Aytac A. Properties of alkali treated short flax fiber reinforced poly(lactic acid)/polycarbonate composites. *Fibers Polym*. 2014;15(12):2607-2612. doi:10.1007/s12221-014-2607-4
17. Keya KN, Kona NA, Koly FA, Maraz KM, Islam MN, Khan RA. Natural fiber reinforced polymer composites: history, types, advantages, and applications. *Mater Eng Res*. 2019;1(2):69-87. doi:10.25082/MER.2019.02.006
18. Usmani MA, Anas M. Study of natural fibre reinforced composites. *IOP Conf Ser Mater Sci Eng*. 2018;404:12048. doi:10.1088/1757-899X/404/1/012048
19. Jiang L, Huang J, Qian J, et al. Study of poly(3-hydroxybutyrate-co-3-hydroxyvalerate) (PHBV)/bamboo pulp fiber composites: effects of nucleation agent and compatibilizer. *J Polym Environ*. 2008;16(2):83-93. doi:10.1007/s10924-008-0086-7
20. Kandola BK, Mistik SI, Pornwannachai W, Horrocks AR. Effects of water and chemical solutions ageing on the physical, mechanical, thermal and flammability properties of natural fibre-reinforced thermoplastic composites. *Molecules*. 2021;26(15):4581. doi:10.3390/molecules26154581
21. Faruk O, Bledzki AK, Fink HP, Sain M. *Biocomposites Reinforced with Natural Fibers: 2000–2010. Prog Polym Sci*. 2012;37(11):1552-1596. doi:10.1016/j.progpolymsci.2012.04.003
22. Rahman MR, Huque MM, Islam MN, Hasan M. Improvement of physico-mechanical properties of jute fiber reinforced polypropylene composites by post-treatment. *Compos Part A: Appl Sci Manuf*. 2008;39(11):1739-1747. doi:10.1016/j.compositesa.2008.08.002
23. Hernández-Díaz D, Villar-Ribera R, Julián F, Tarrés Q, Espinach FX, Delgado-Aguilar M. Topography of the interfacial shear strength and the mean intrinsic tensile strength of hemp fibers as a reinforcement of polypropylene. *Materials*. 2020;13(4):1012. doi:10.3390/ma13041012
24. Defoirdt N, Biswas S, Vriese LD, et al. Assessment of the tensile properties of coir, bamboo and jute fibre. *Compos Part A: Appl Sci Manuf*. 2010;41(5):588-595. doi:10.1016/j.compositesa.2010.01.005
25. le Duigou A, Bourmaud A, Balnois E, Davies P, Baley C. Improving the interfacial properties between flax fibres and

15480569, 2025, 8, Downloaded from https://4spepublications.onlinelibrary.wiley.com/doi/10.1002/pc.29460 by Turkey Cochrane Evidence Aid, Wiley Online Library on [06/06/2026]. See the Terms and Conditions (https://onlinelibrary.wiley.com/terms-and-conditions) on Wiley Online Library for rules of use; OA articles are governed by the applicable Creative Commons License

PLLA by a water fibre treatment and drying cycle. *Ind Crop Prod*. 2012;39:31-39. doi:10.1016/j.indcrop.2012.02.001
26. Le Duigou A, Correa D, Ueda M, Matsuzaki R, Castro M. A review of 3D and 4D printing of natural fibre biocomposites. *Mater Des*. 2020;194:108911. doi:10.1016/j.matdes.2020.108911
27. Deb D, Jafferson JM. Natural fibers reinforced FDM 3D printing filaments. *Mater Today Proc*. 2021;46:1308-1318. doi:10.1016/j.matpr.2021.02.397
28. Amaducci S, Scordia D, Liu FH, et al. Key cultivation techniques for hemp in Europe and China. *Ind Crop Prod*. 2015;68:2-16. doi:10.1016/j.indcrop.2014.06.041
29. Liu M, Thygesen A, Summerscales J, Meyer AS. Targeted pretreatment of hemp bast fibres for optimal performance in biocomposite materials: a review. *Ind Crop Prod*. 2017;108:660-683. doi:10.1016/j.indcrop.2017.07.027
30. Gebler M, Schoot Uiterkamp AJM, Visser C. A global sustainability perspective on 3D printing technologies. *Energy Policy*. 2014;74:158-167. doi:10.1016/j.enpol.2014.08.033
31. Perkins I, Skitmore M. Three-dimensional printing in the construction industry: a review. *Int J Constr Manag*. 2015;15(1):1-9. doi:10.1080/15623599.2015.1012136
32. Khan SA, Koç M, Al-Ghamdi SG. Sustainability assessment, potentials and challenges of 3D printed concrete structures: a systematic review for built environmental applications. *J Clean Prod*. 2021;303:127027. doi:10.1016/j.jclepro.2021.127027
33. Marijnissen MPAM, Van Der Zee A. 3D Concrete Printing in Architecture A Research on the Potential Benefits of 3D Concrete Printing in Architecture. *Mater Stud-Method*. 2017;2:299-308. doi:10.52842/conf.ecaade.2017.2.299
34. Siddika A, Al Mamun MA, Ferdous W, Saha AK, Alyousef R. 3D-printed concrete: applications, performance, and challenges. *J Sustain Cem-Based Mater*. 2020;9(3):127-164. doi:10.1080/21650373.2019.1705199
35. Hotza D, Gomes CM, Günster J. Advances in additive manufacturing processes and materials. *Adv Mech Eng*. 2014;6:645075. doi:10.1155/2014/645075
36. Sabbatini B, Cambriani A, Cespi M, Palmieri GF, Perinelli DR, Bonacucina G. An overview of natural polymers as reinforcing agents for 3D printing. *Chem Eng*. 2021;5(4):78. doi:10.3390/chemengineering5040078
37. Mazzanti V, Malagutti L, Mollica F. FDM 3D printing of polymers containing natural fillers: a review of their mechanical properties. *Polymers (Basel)*. 2019;11(7):1094. doi:10.3390/polym11071094
38. Oksman K, Skrifvars M, Selin J-F. Natural fibres as reinforcement in polylactic acid (PLA) composites. *Compos Sci Technol*. 2003;63(9):1317-1324. doi:10.1016/S0266-3538(03)00103-9
39. Stoof D, Pickering K. Sustainable composite fused deposition modelling filament using recycled pre-consumer polypropylene. *Compos B: Eng*. 2018;135:110-118. doi:10.1016/j.compositesb.2017.10.005
40. Milosevic M, Stoof D, Pickering K. Characterizing the mechanical properties of fused deposition modelling natural fiber recycled polypropylene composites. *J Compos Sci*. 2017;1(1):7. doi:10.3390/jcs1010007
41. Appusamy AM, Nanjappan N, Eswaran P, Subramanian M. The effect of natural Gongura roselle fiber on the mechanical properties of 3D printed ABS and PLA composites. *Polimery*. 2022;67(3):119-124. doi:10.14314/polimery.2022.3.4
42. Depuydt D, Balthazar M, Hendrickx K, et al. Production and characterization of bamboo and flax fiber reinforced polylactic acid filaments for fused deposition modeling (FDM). *Polym Compos*. 2019;40(5):1951-1963. doi:10.1002/pc.24971
43. Osman MA, Atia MRA. Investigation of ABS-rice straw composite feedstock filament for FDM. *Rapid Prototyp J*. 2018;24(6):1067-1075. doi:10.1108/RPJ-11-2017-0242
44. Šafka J, Ackermann M, Bobek J, Seidl M, Habr J, Běhálek L. Use of composite materials for FDM 3D print technology. *Mater Sci Forum*. 2016;862:174-181. doi:10.4028/www.scientific.net/MSF.862.174
45. Torrado AR, Shemelya CM, English JD, Lin Y, Wicker RB, Roberson DA. Characterizing the effect of additives to ABS on the mechanical property anisotropy of specimens fabricated by material extrusion 3D printing. *Addit Manuf*. 2015;6:16-29. doi:10.1016/j.addma.2015.02.001
46. Torrado Perez AR, Roberson DA, Wicker RB. Fracture surface analysis of 3D-printed tensile specimens of novel ABS-based materials. *J Fail Anal Prev*. 2014;14(3):343-353. doi:10.1007/s11668-014-9803-9
47. Ahmad MN, Wahid MK, Maidin NA, Ab Rahman MH, Osman MH, Alis@Elias IF. Mechanical characteristics of oil palm fiber reinforced thermoplastics as filament for fused deposition modeling (FDM). *Adv Manuf*. 2020;8(1):72-81. doi:10.1007/s40436-019-00287-w
48. Marton AMS, Monticeli FM, Zanini NC, et al. Revalorization of Australian royal palm (Archontophoenix alexandrae) waste as reinforcement in acrylonitrile butadiene styrene (ABS) for use in 3D printing pen. *J Clean Prod*. 2022;365:132808. doi:10.1016/j.jclepro.2022.132808
49. Agaliotis EM, Ake-Concha BD, May-Pat A, et al. Tensile behavior of 3D printed polylactic acid (PLA) based composites reinforced with natural fiber. *Polymers (Basel)*. 2022;14(19):3976. doi:10.3390/polym14193976
50. Figueroa-Velarde V, Diaz-Vidal T, Cisneros-López EO, et al. Mechanical and physicochemical properties of 3D-printed agave fibers/poly(lactic) acid biocomposites. *Materials*. 2021;14(11):3111. doi:10.3390/ma14113111
51. Liu H, He H, Peng X, Huang B, Li J. Three-dimensional printing of poly(lactic acid) bio-based composites with sugarcane bagasse fiber: effect of printing orientation on tensile performance. *Polym Adv Technol*. 2019;30(4):910-922. doi:10.1002/pat.4524
52. Zhao DX, Cai X, Shou GZ, Gu YQ, Wang PX. Study on the preparation of bamboo plastic composite intend for additive manufacturing. *Key Eng Mater*. 2015;667:250-258. doi:10.4028/www.scientific.net/KEM.667.250
53. Matsuzaki R, Ueda M, Namiki M, et al. Three-dimensional printing of continuous-fiber composites by in-nozzle impregnation. *Sci Rep*. 2016;6(1):23058. doi:10.1038/srep23058
54. Stoof D, Pickering K, Zhang Y. Fused deposition modelling of natural fibre/polylactic acid composites. *J Compos Sci*. 2017;1(1):8. doi:10.3390/jcs1010008
55. Vidakis N, Petousis M, Velidakis E, Spiridaki M, Kechagias JD. Mechanical performance of fused filament fabricated and 3D-printed polycarbonate polymer and

15480569, 2025, 8, Downloaded from https://4spepublications.onlinelibrary.wiley.com/doi/10.1002/pc.29460 by Turkey Cochrane Evidence Aid, Wiley Online Library on [06/06/2026]. See the Terms and Conditions (https://onlinelibrary.wiley.com/terms-and-conditions) on Wiley Online Library for rules of use; OA articles are governed by the applicable Creative Commons License

polycarbonate/cellulose nanofiber nanocomposites. *Fibers*. 2021;9(11):74. doi:10.3390/fib9110074

56. Vidakis N, Petousis M, Kechagias JD. A comprehensive investigation of the 3D printing parameters' effects on the mechanical response of polycarbonate in fused filament fabrication. *Prog Addit Manuf*. 2022;7(4):713-722. doi:10.1007/s40964-021-00258-3
57. Vinyas M, Athul S, Harursampath D, Nguyen Thoi T. Experimental evaluation of the mechanical and thermal properties of 3D printed PLA and its composites. *Mater Res Express*. 2019;6(11):115301. doi:10.1088/2053-1591/ab43ab
58. Liang GG, Cook WD, Tcharkhtchi A, Sautereau H. Epoxy as a reactive plasticizer for improving polycarbonate processibility. *Eur Polym J*. 2011;47(8):1578-1588. doi:10.1016/j.eurpolymj.2011.05.005
59. Tofail SAM, Koumoulos EP, Bandyopadhyay A, Bose S, O'Donoghue L, Charitidis C. Additive manufacturing: scientific and technological challenges, market uptake and opportunities. *Mater Today*. 2018;21(1):22-37. doi:10.1016/j.mattod.2017.07.001
60. Jiang S, Guan R, Chen H, Zhao J, Zha S, Ke Z. Effect of TBC plasticization on thin polycarbonate sheet. *J Wuhan Univ Technol Mater Sci ed*. 2014;29(3):553-560. doi:10.1007/s11595-014-0956-x
61. Pawlowski KH, Schartel B. Flame retardancy mechanisms of triphenyl phosphate, resorcinol bis(diphenyl phosphate) and bisphenol a bis(diphenyl phosphate) in polycarbonate/acrylonitrile–butadiene–styrene blends. *Polym Int*. 2007;56(11):1404-1414. doi:10.1002/pi.2290
62. van der Veen I, de Boer J. Phosphorus flame retardants: properties, production, environmental occurrence, toxicity and analysis. *Chemosphere*. 2012;88(10):1119-1153. doi:10.1016/j.chemosphere.2012.03.067
63. Hörold S. Phosphorus-based and intumescent flame retardants. *Polymer Green Flame Retardants*. Elsevier; 2014:221-254. doi:10.1016/B978-0-444-53808-6.00006-8
64. Jang BN, Wilkie CA. The effects of triphenylphosphate and recorcinolbis(diphenylphosphate) on the thermal degradation of polycarbonate in air. *Thermochim Acta*. 2005;433(1–2):1-12. doi:10.1016/j.tca.2005.01.071
65. World Health Organization. *ENVIRONMENTAL HEALTH CRITERIA 111 Triphenyl Phosphate*. World Health Organization; 1991.
66. Menčík P, Přikryl R, Stehnová I, et al. Effect of selected commercial plasticizers on mechanical, thermal, and morphological properties of poly(3-hydroxybutyrate)/poly(lactic acid)/plasticizer biodegradable blends for three-dimensional (3D) print. *Materials*. 2018;11(10):1893. doi:10.3390/ma11101893
67. Jung HC, Kim WN, Lee CR, Suh KS, Kim S-R. Properties of flame-retarding blends of polycarbonate and poly(acrylonitrile-butadiene-styrene). *J Polym Eng*. 1998;18(1–2):115-130. doi:10.1515/polyeng-1998-1-210
68. Lei C, Chen D. Effect of di- *n* -dodecyl phosphate on the transesterification reaction in a poly(butylene terephthalate)/polycarbonate blend. *J Appl Polym Sci*. 2008;109(2):1099-1104. doi:10.1002/app.28060
69. Feyz E, Jahani Y, Esfandeh M, Ghafelehbashi M, Jafari SH. Study of the viscoelastic properties of PC/ABS blend containing triphenyl phosphate and nanoclay and its correlation with morphology. *J Appl Polym Sci*. 2010;118(3):1796-1804. doi:10.1002/app.32544
70. Swoboda B, Buonomo S, Leroy E, Lopez Cuesta JM. Fire retardant poly(ethylene terephthalate)/polycarbonate/triphenyl phosphite blends. *Polym Degrad Stab*. 2008;93(5):910-917. doi:10.1016/j.polymdegradstab.2008.02.003
71. Bajwa D, Eichers M, Shojaeiarani J, Kallmeyer A. Influence of biobased plasticizers on 3D printed polylactic acid composites filled with sustainable biofiller. *Ind Crop Prod*. 2021;173:114132. doi:10.1016/j.indcrop.2021.114132
72. Coppola B, Garofalo E, Di Maio L, Scarfato P, Incarnato L. Investigation on the use of PLA/hemp composites for the fused deposition modelling (FDM) 3D printing. 2018;020086. doi:10.1063/1.5045948
73. Ceylan İ, Çakıcı Alp N, Aytaç A. Sustainable 3D printing with alkali-treated hemp fiber-reinforced polycarbonate composites. *Cellulose*. 2024;31:4477-4495. doi:10.1007/s10570-024-05904-x
74. Pandzic A, Hodzic D, Milovanovic A. Effect of infill type and density on tensile properties of PLA material for FDM process, 30th DAAAM International Symposium on Intelligent Manufacturing and Automation, pp. 545–554. 2019. doi:10.2507/30th.daaam.proceedings.074
75. Peraro J. *Limitations of Test Methods for Plastics*. ASTM International. 2000. doi:10.1520/STP1369-EB
76. ISO 4589-2. *Plastics — Determination of burning behaviour by oxygen index*. 2017 www.iso.orgiTehSTANDARDPREVIEW
77. ASTM D, 635. *Standard Test Method for Rate of Burning and/or Extent and Time of Burning of Plastics in a Horizontal Position*. ASTM International: West Conshohocken; 2003.
78. Feng J, Hao J, Du J, Yang R. Using TGA/FTIR TGA/MS and cone calorimetry to understand thermal degradation and flame retardancy mechanism of polycarbonate filled with solid bisphenol a bis(diphenyl phosphate) and montmorillonite. *Polym Degrad Stab*. 2012;97(4):605-614. doi:10.1016/j.polymdegradstab.2012.01.011
79. Jang BN, Wilkie CA. A TGA/FTIR and mass spectral study on the thermal degradation of bisphenol a polycarbonate. *Polym Degrad Stab*. 2004;86(3):419-430. doi:10.1016/j.polymdegradstab.2004.05.009
80. Reddy BM, Mohana Reddy YV, Mohan Reddy BC, Reddy RM. Mechanical, morphological, and thermogravimetric analysis of alkali-treated Cordia-Dichotoma natural fiber composites. *J Nat Fibers*. 2020;17(5):759-768. doi:10.1080/15440478.2018.1534183
81. Apaydin-Varol E, Polat S, Putun AE. Pyrolysis kinetics and thermal decomposition behavior of polycarbonate - a TGA-FTIR study. *Therm Sci*. 2014;18(3):833-842. doi:10.2298/TSCI1403833A
82. Haghighi-Yazdi M, Lee-Sullivan P. FTIR analysis of a polycarbonate blend after hygrothermal aging. *J Appl Polym Sci*. 2015;132(3):41316. doi:10.1002/app.41316
83. Xu JZ, Gao M, Guo HZ, et al. Study on the thermal degradation of cellulosic fibers treated with flame retardants. *J Fire Sci*. 2002;20(3):227-235. doi:10.1177/0734904102020003905
84. Shao L, Xu B, Ma W, Wang J, Liu Y, Qian L. Flame retardant application of a hypophosphite/cyclotetrasiloxane bigroup compound on polycarbonate. *J Appl Polym Sci*. 2020;137(14):48699. doi:10.1002/app.48699
85. Islam MS, Pickering KL, Foreman NJ. Influence of alkali treatment on the interfacial and physico-mechanical

15480569, 2025, 8, Downloaded from https://4spepublications.onlinelibrary.wiley.com/doi/10.1002/pc.29460 by Turkey Cochrane Evidence Aid, Wiley Online Library on [06/06/2026]. See the Terms and Conditions (https://onlinelibrary.wiley.com/terms-and-conditions) on Wiley Online Library for rules of use; OA articles are governed by the applicable Creative Commons License

properties of industrial hemp fibre reinforced polylactic acid composites. *Compos Part A: Appl Sci Manuf*. 2010;41(5):596-603. doi:10.1016/j.compositesa.2010.01.006

86. Xiao HW, Li P, Ren X, Jiang T, Yeh J. Isothermal crystallization kinetics and crystal structure of poly(lactic acid): effect of triphenyl phosphate and talc. *J Appl Polym Sci*. 2010;118(6):3558-3569. doi:10.1002/app.32728
87. Twite-Kabamba E, Mechraoui A, Rodrigue D. Rheological properties of polypropylene/hemp fiber composites. *Polym Compos*. 2009;30(10):1401-1407. doi:10.1002/pc.20704
88. Jang K-S. Mechanics and rheology of basalt fiber-reinforced polycarbonate composites. *Polymer (Guildf)*. 2018;147:133-141. doi:10.1016/j.polymer.2018.06.004
89. Wypych G. *Handbook of Plasticizers*. ChemTec Publications; William Andrew Publications; 2004.
90. Shaikh H, Alothman OY, Alshammari BA, Jawaid M. Dynamic and thermo-mechanical properties of polypropylene reinforced with date palm nano filler. *J King Saud Univ Sci*. 2023;35(3):102561. doi:10.1016/j.jksus.2023.102561
91. Nayak SK, Mohanty S, Samal SK. Influence of short bamboo/glass fiber on the thermal, dynamic mechanical and rheological properties of polypropylene hybrid composites. *Mater Sci Eng A*. 2009;523(1–2):32-38. doi:10.1016/j.msea.2009.06.020
92. Threepopnatkul P, Kaerkitcha N, Athipongarporn N. Effect of surface treatment on performance of pineapple leaf fiber–polycarbonate composites. *Compos B: Eng*. 2009;40(7):628-632. doi:10.1016/j.compositesb.2009.04.008
93. Yan C, Xu B, Shan D, et al. Fabrication and mechanism research of high-efficiency water-resistant flame retardant, transparent and mechanically reinforced polycarbonate composites. *Polym Test*. 2023;119:107937. doi:10.1016/j.polymertesting.2023.107937
94. Del Rey R, Serrat R, Alba J, Perez I, Mutje P, Espinach F. Effect of sodium hydroxide treatments on the tensile strength and the interphase quality of hemp Core fiber-reinforced polypropylene composites. *Polymers (Basel)*. 2017;9(8):377. doi:10.3390/polym9080377
95. Zhou Y, Zou J, Wu H, Xu B. Balance between bonding and deposition during fused deposition modeling of polycarbonate and acrylonitrile-butadiene-styrene composites. *Polym Compos*. 2020;41(1):60-72. doi:10.1002/pc.25345
96. Zhang C, Yang R, Li X, Yi D. Preparation of polystyrene/triphenyl phosphate composites by suspension polymerization and melt extrusion method — a comparative study. *Chin J Polym Sci*. 2016;34(6):688-696. doi:10.1007/s10118-016-1791-7
97. Jalalah M, Zulfiqar S, Afzal A, et al. Microencapsulation based fire retardant eco-friendly jute composite. *Polym Polym Compos*. 2023;31:096739112211477. doi:10.1177/09673911221147702
98. Fekete I, Ronkay F, Lendvai L. Highly toughened blends of poly(lactic acid) (PLA) and natural rubber (NR) for FDM-based 3D printing applications: the effect of composition and infill pattern. *Polym Test*. 2021;99:107205. doi:10.1016/j.polymertesting.2021.107205
99. Ji A, Zhang S, Bhagia S, Yoo CG, Ragauskas AJ. 3D printing of biomass-derived composites: application and characterization approaches. *RSC Adv*. 2020;10(37):21698-21723. doi:10.1039/D0RA03620J
100. Yemisci F, Yesil S, Aytac A. Improvement of the flame retardancy of plasticized poly(lactic acid) by means of phosphorus-based flame retardant fillers. *Fire Mater*. 2017;41(8):964-972. doi:10.1002/fam.2440
101. Hazer S, Coban M, Aytac A. Effects of ammonium polyphosphate and triphenyl phosphate on the flame retardancy, thermal, and mechanical properties of glass fiber–reinforced PLA/PC composites. *Fire Mater*. 2019;43(3):277-282. doi:10.1002/fam.2696

How to cite this article: Ceylan Engin I, Cakici Alp N, Aytac A. Evaluation of the effect of triphenyl phosphate on hemp fiber-reinforced polycarbonate composites for 3D printing applications. *Polym Compos*. 2025;46(8):7717-7733. doi:10.1002/pc.29460

15480569, 2025, 8, Downloaded from https://4spepublications.onlinelibrary.wiley.com/doi/10.1002/pc.29460 by Turkey Cochrane Evidence Aid, Wiley Online Library on [06/06/2026]. See the Terms and Conditions (https://onlinelibrary.wiley.com/terms-and-conditions) on Wiley Online Library for rules of use; OA articles are governed by the applicable Creative Commons License